SICE Annual Conference 2011
September 13-18, 2011, Waseda University, Tokyo, Japan

Energy Efficiency Rate Optimization of Bracing Robot

Michiyuki Itoshima[1], Yusuke Toda[1], Tomohide Maeba[1], Hidemi Kataoka[1],
Mamoru Minami[1] and Akira Yanou[1]

[1]Graduate School of Natural Science and Technology, Okayama University, Okayama, Japan
(Tel: +81-86-251-8924; E-mail: itoshima@suri.sys.okayama-u.ac.jp)

Abstract: This paper researches on finding better position in motion control of robot with elbow attaching to environment as a bracing, where the robots hand is required to track a desired trajectory and to maximum energy efficiency. Considering that human can do accurate task with small powers by contacting elbow or wrist on a table, we thought that manipulators can save energy and do a task more precisely like human by bracing itself. Therefore this paper discusses the motion equation of robot under bracing condition, based on the robot's dynamics with constraint condition including the motor's dynamics. Then, we evaluate the performance from the two points of view, energy efficiency and trajectory tracking accuracy, the best position of contacting point has been found by simulations.

Keywords: Constraint motion, Energy efficiency, Dynamical model

1. INTRODUCTION

Robot that can shape complex configuration is used at various situations now. If the robot's redundancy increases, the robot can work on objects with complicated structure because it has many links and can shape complex configuration. However, the more number of links increases, the more manipulator's weight and dynamic interference between links increase. Therefore, the control accuracy of end-effector worsens, and then the bigger power and energy will be needed in order to control the robot's hand trajectory accurately. Considering that human can fulfill accurate task with small powers by contacting elbow on a table as shown Fig. **??**, we believe that manipulators can save energy and can do a task more precisely like human by bracing itself. So we think if such motion can be applied into robots, it can help the robots' application such as rescue robot and other manipulators improve the performances.

Then, in this paper we compare the motion of robot contacting its elbow on the table with non-contacting robot's motion concerning accuracy to show that contacting elbow on the table achieves high trajectory tracking accuracy and high energy efficiency. We concentrate in this paper our discussion on whether a best contacting position of the elbow that maximizes the energy efficiency and the trajectory tracking accuracy exists or not. As a precondition of the evaluation of this bracing motion, we included an existence of a friction force at the bracing point, and also included all motions' dynamics concerning electric currents and input voltages used for estimating electric energy consumption. With the robot's motion evaluated from the accuracy of the hand trajectory tracking and energy consumption efficiency, we found that almost the same bracing motion assures the highest tracking accuracy and also highest energy efficiency.

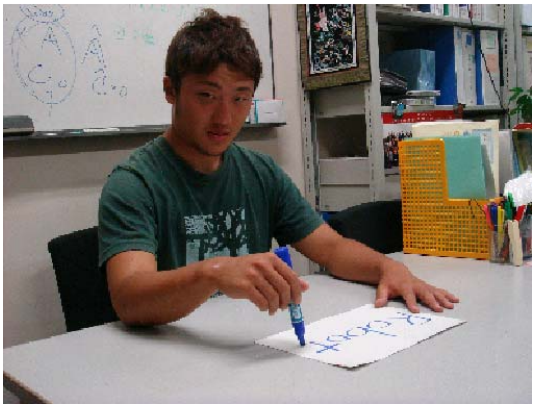

Fig. 1 Writing motion

2. MODELING WITH CONSTRAINT CONDITION

2.1 Equation of Motion with Constraint Condition

To make the explanation of constraint motion with multi-elbow be easily understandable, we discuss firstly about the model of the manipulator whose end-effector is contacing rigid environment without elasticity. Equation of motion of manipulator composing rigid structure of l links, and also contact relation between manipulator's end-effector and definition of constraint surface should be introduced firstly.

The manipulator's model with constraint is shown in Fig.2. From Fig.2, the equation of motion with constraint condition can be expressed as follows.

$$\begin{aligned} &\boldsymbol{M}(\boldsymbol{q})\ddot{\boldsymbol{q}} + \boldsymbol{h}(\boldsymbol{q}, \dot{\boldsymbol{q}}) + \boldsymbol{g}(\boldsymbol{q}) + \boldsymbol{D}(\dot{\boldsymbol{q}}) \\ &= \boldsymbol{\tau} + \left(\frac{\partial C}{\partial \boldsymbol{q}^T}\right)^T \left(f_n / \left\| \frac{\partial C}{\partial \boldsymbol{r}^T} \right\|\right) - \left(\frac{\partial \boldsymbol{r}}{\partial \boldsymbol{q}^T}\right)^T \frac{\dot{\boldsymbol{r}}}{\|\dot{\boldsymbol{r}}\|} f_t \end{aligned} \quad (1)$$

$\boldsymbol{M}$ is $l \times l$ inertia matrix, $\boldsymbol{h}$ and $\boldsymbol{g}$ are $l \times 1$ vectors which indicate the effects from Coriolis force, centrifugal force and gravity. $\boldsymbol{D}$ is $l \times l$ diagonal matrix of coefficients of joint's viscous friction. $\boldsymbol{q}$ is joint angle and $\boldsymbol{\tau}$ is input torque. f_n is constraint force and f_t is friction force.

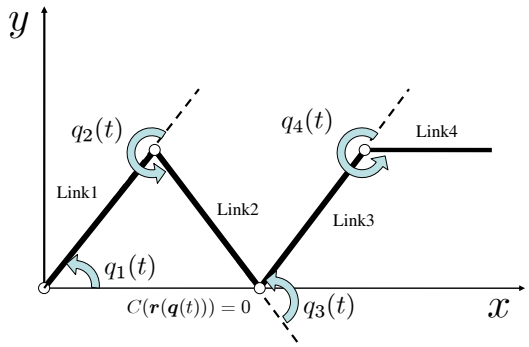

Fig. 2 Manipulator's model with constraint

Here, we set two assumptions: (i) f_n and f_t are orthogonal. (ii) $f_t = Kf_n$ (K is proportional constant).

And, C included in Eq (1) is an expression of constraint surface, and the relation expressed in Eq (2) is constraint condition.

$$C(\boldsymbol{r}(\boldsymbol{q}(t))) = 0 \tag{2}$$

Eq (2) is the equation realized constraint, and $\boldsymbol{r}(\boldsymbol{q}(t))$ means the coordinates with constraint link's point. Moreover, Eq (2) is differentiated by time t two times, and then we can derive the constraint condition of $\ddot{\boldsymbol{q}}$. In real control, it needs constraint on acceleration of level.

$$\Big[\frac{\partial}{\partial \boldsymbol{q}^T}\Big(\frac{\partial C}{\partial \boldsymbol{q}^T}\Big)\dot{\boldsymbol{q}}\Big]\dot{\boldsymbol{q}} + \Big(\frac{\partial C}{\partial \boldsymbol{q}^T}\Big)\ddot{\boldsymbol{q}} = 0 \tag{3}$$

If the coefficients of f_n and f_t are defined as $\boldsymbol{j}_c^T$ and $\boldsymbol{j}_t^T$,

$$\boldsymbol{j}_c^T = \Big(\frac{\partial C}{\partial \boldsymbol{q}^T}\Big)^T / \Big\|\frac{\partial C}{\partial \boldsymbol{r}}\Big\| \tag{4}$$

$$\boldsymbol{j}_t^T = \left(\frac{\partial \boldsymbol{r}}{\partial \boldsymbol{q}^T}\right)^T \frac{\dot{\boldsymbol{r}}}{\|\dot{\boldsymbol{r}}\|} \tag{5}$$

Considering about constraint of the intermediate links, the manipulator's equation of motion can be expressed as

$$\begin{aligned}&\boldsymbol{M}(\boldsymbol{q})\ddot{\boldsymbol{q}} + \boldsymbol{h}(\boldsymbol{q}, \dot{q}) + \boldsymbol{g}(\boldsymbol{q}) + \boldsymbol{D}\dot{q} \\ &= \boldsymbol{\tau} + \boldsymbol{j}_c^T f_n - \boldsymbol{j}_t^T f_t\end{aligned} \tag{6}$$

where f_n is a reaction force exerting from constraint surface to the robot's elbow, and f_t is a friction force acting on the same point. To make sure that manipulator's elbow is contacting with the constraint surface all the time, value of $\boldsymbol{q}(t)$ in Eq (6) has always to satisfy Eq (2) whenever the time t has any value. For assuring that the solution $\boldsymbol{q}(t)$ of Eq (6) showed satisfy the constraint Eq (2) despite any time t, the value of $\ddot{\boldsymbol{q}}$ in Eq (3) should have the same value with $\ddot{\boldsymbol{q}}$ in Eq (6), then value of $\boldsymbol{q}(t)$ in Eq (6) and Eq (2) necessarily always keep the same regardless of time.

2.2 Robot Dynamics including Motor

In this research, we want to evaluate effects on increasing trajectory tracking accuracy and reducing energy consumption used for countering the gravity force and other effects by bracing the intermediate link. Even though there is no robot's motion - - -robot is stopping- - - the energy is kept to be consuming since motors of joints have to generate torques to maintain the required robot's configuration against gravity influences. When the robot is in motion, other effects of dynamics will be added more to the gravity effect. To evaluate this kind of wasted energy consumption, we included the effects of electronic circuit flowing in servo motors into the equation of motion of the manipulator to represent explicitly that the robot consumes energy even while stopping.

For $i = 1, 2, 3, 4$, equation of voltage, counter electromotive force, equation of motion and generation of torque can be expressed as follows.

$$v_i(t) = L_i\dot{i}_i + R_i i_i(t) + v_{gi}(t) \tag{7}$$

$$v_{gi}(t) = K_{Ei}\dot{\theta}_i(t) \tag{8}$$

$$I_{mi}\ddot{\theta}_i = \tau_{gi}(t) - \tau_{Li}(t) - d_{mi}\dot{\theta}_i \tag{9}$$

$$\tau_g(t) = K_{Ti} i_i(t) \quad (i = 1, 2, 3, 4) \tag{10}$$

v_i is terminal voltage of motor, R_i, electrical resistance, L_i, inductance, i_i, electric current flowing through a circuit, θ_i, angular displacement of motor, τ_{gi}, generation of torque, τ_{Li}, load torque, v_i, counter electromotive force, I_{mi}, moment of inertia of motor, K_{Ei}, constant of counter electromotive force, K_{Ti}, torque constant, d_{mi}, coefficient of viscous friction of decelerator.

From the relation of magnetic field and the coefficients above, $K_{Ti} = K_{Ei}(= K)$ holds for motors used. Combine Eq (8) and Eq (7), and also Eq (10) and Eq (9), we derive

$$v_i = L_i\dot{i}_i + R_i i_i + K_i\dot{\theta}_i \tag{11}$$

$$I_{mi}\ddot{\theta}_i = K_i i_i - \tau_{Li} - d_{mi}\dot{\theta}_i \tag{12}$$

In the situation with motor and gear whose gear ratio is $k_i > 1$ are installed onto manipulator,

$$\theta_i = k_i q_i \tag{13}$$

$$\tau_{Li} = \frac{\tau_i}{k_i} \tag{14}$$

Combining Eq (11) and Eq (12) into equation with $\dot{i}_i$ and τ_i, following equations are obtained

$$L_i\dot{i}_i = v_i - R_i i_i - K_i k_i \dot{q}_i \tag{15}$$

$$\tau_i = -I_{mi}k_i^2\ddot{q}_i + K_i k_i i_i - d_{mi}k_i^2\dot{q}_i \tag{16}$$

Then using vector and matrix to indicate Eq (15) and (16),

$$\boldsymbol{L}\dot{\boldsymbol{i}} = \boldsymbol{v} - \boldsymbol{R}\boldsymbol{i} - \boldsymbol{K_m}\dot{\boldsymbol{q}} \tag{17}$$

$$\boldsymbol{\tau} = -\boldsymbol{J_m}\ddot{\boldsymbol{q}} + \boldsymbol{K_m}\boldsymbol{i} - \boldsymbol{D_m}\dot{\boldsymbol{q}} \tag{18}$$

$$\boldsymbol{v} = [v_1, v_2, \cdots, v_s]^T$$

$$\boldsymbol{i} = [i_1, i_2, \cdots, i_s]^T$$

and the definitions are shown as follow, which always

have positive value.

$$\begin{aligned}
\boldsymbol{L} &= diag[L_1, L_2, \cdots, L_s] \\
\boldsymbol{R} &= diag[R_1, R_2, \cdots, R_s] \\
\boldsymbol{K_m} &= diag[K_{m1}, K_{m2}, \cdots, K_{ms}] \\
\boldsymbol{J_m} &= diag[J_{m1}, J_{m2}, \cdots, J_{ms}] \\
\boldsymbol{D_m} &= diag[D_{m1}, D_{m2}, \cdots, D_{ms}] \\
K_{mi} &= K_i k_i,\ J_{mi} = I_{mi} k_i^2,\ D_{mi} = d_{mi} k_i^2
\end{aligned}$$

Now substitute Eq (18) into Eq (6), we get

$$\begin{aligned}
&(\boldsymbol{M}(\boldsymbol{q}) + \boldsymbol{J_m})\ddot{\boldsymbol{q}} + \boldsymbol{h}(\boldsymbol{q}, \dot{\boldsymbol{q}}) + \boldsymbol{g}(\boldsymbol{q}) + (\boldsymbol{D} + \boldsymbol{D_m})\dot{\boldsymbol{q}} \\
&= \boldsymbol{K_m i} + \boldsymbol{j_c}^T f_n - \boldsymbol{j_t}^T f_t
\end{aligned} \tag{19}$$

Similar to the same relation between Eq (6) and Eq (3), the value of $\ddot{\boldsymbol{q}}$ in Eq (19) have to be identical to the value of $\ddot{\boldsymbol{q}}$ in Eq (3) representing constrain condition.

2.3 Robot/Motor Equation with Contact Constraint

To make sure that $\ddot{\boldsymbol{q}}$ in Eq (19) and (3) be identical, constraint force f_n is subordinately decided by simultaneous equation. With an assumption $f_t = K f_n$ considering, Eq (19),(3) should be transformed as follow

$$\begin{aligned}
&(\boldsymbol{M}(\boldsymbol{q}) + \boldsymbol{J_m})\ddot{\boldsymbol{q}} - \boldsymbol{j_c}^T f_n + \boldsymbol{j_t}^T K f_n \\
&= \boldsymbol{K_m i} - \boldsymbol{h} - \boldsymbol{g} - (\boldsymbol{D} + \boldsymbol{D_m})\dot{\boldsymbol{q}}
\end{aligned} \tag{20}$$

$$\begin{aligned}
(\frac{\partial C}{\partial \boldsymbol{q}^T})\ddot{\boldsymbol{q}} &= -\left[\frac{\partial}{\partial \boldsymbol{q}}(\frac{\partial C}{\partial \boldsymbol{q}})\dot{\boldsymbol{q}}\right]\dot{\boldsymbol{q}} \\
&= -\dot{\boldsymbol{q}}^T\left[\frac{\partial}{\partial \boldsymbol{q}}(\frac{\partial C}{\partial \boldsymbol{q}^T})\right]\dot{\boldsymbol{q}}
\end{aligned} \tag{21}$$

Then Eq (20),(21),(17) can be expressed as follow,

$$\begin{aligned}
&\begin{bmatrix} \boldsymbol{M} + \boldsymbol{J_m} & -(\boldsymbol{j_c}^T - \boldsymbol{j_t}^T K) & \boldsymbol{0} \\ \frac{\partial C}{\partial \boldsymbol{q}^T} & 0 & \boldsymbol{0} \\ \boldsymbol{0} & \boldsymbol{0} & \boldsymbol{L} \end{bmatrix} \begin{bmatrix} \ddot{\boldsymbol{q}} \\ f_n \\ \dot{\boldsymbol{i}} \end{bmatrix} \\
&= \begin{bmatrix} \boldsymbol{K_m i} - \boldsymbol{h} - \boldsymbol{g} - (\boldsymbol{D} + \boldsymbol{D_m})\dot{\boldsymbol{q}} \\ -\dot{\boldsymbol{q}}^T\left[\frac{\partial}{\partial \boldsymbol{q}}(\frac{\partial C}{\partial \boldsymbol{q}^T})\right]\dot{\boldsymbol{q}} \\ \boldsymbol{v} - \boldsymbol{R i} - \boldsymbol{K_m}\dot{\boldsymbol{q}} \end{bmatrix}
\end{aligned} \tag{22}$$

Furthermore by redefining as

$$\boldsymbol{M}^* = \begin{bmatrix} \boldsymbol{M} + \boldsymbol{J_m} & -(\boldsymbol{j_c}^T - \boldsymbol{j_t}^T K) & \boldsymbol{0} \\ \frac{\partial C}{\partial \boldsymbol{q}^T} & 0 & 0 \\ \boldsymbol{0} & \boldsymbol{0} & \boldsymbol{L} \end{bmatrix} \tag{23}$$

$$\boldsymbol{b} = \begin{bmatrix} \boldsymbol{K_m i} - \boldsymbol{h} - \boldsymbol{g} - (\boldsymbol{D} + \boldsymbol{D_m})\dot{\boldsymbol{q}} \\ -\dot{\boldsymbol{q}}^T\left[\frac{\partial}{\partial \boldsymbol{q}}(\frac{\partial C}{\partial \boldsymbol{q}^T})\right]\dot{\boldsymbol{q}} \\ \boldsymbol{v} - \boldsymbol{R i} - \boldsymbol{K_m}\dot{\boldsymbol{q}} \end{bmatrix} \tag{24}$$

Then Eq (22) can be expressed as

$$\boldsymbol{M}^* \begin{bmatrix} \ddot{\boldsymbol{q}} \\ f_n \\ \dot{\boldsymbol{i}} \end{bmatrix} = \boldsymbol{b} \tag{25}$$

$\boldsymbol{M}^*$ has been confirmed to be nonsingular matrix so for through many numerical simulations, it has to be power by mathematical procedures. Through calculating $\boldsymbol{M}^*$, the unknown value of $\ddot{\boldsymbol{q}}$, $\boldsymbol{f_n}$,$\dot{\boldsymbol{i}}$ can be determined based on the above simultaneous equation.

3. FORWARD DYNAMICS CALCULATION

To calculate $\boldsymbol{M}^*$, $\boldsymbol{b}$ in Eq (25), we need to first calculate $\boldsymbol{M}$, $\boldsymbol{h}$, $\boldsymbol{g}$. Here we can notice that $\boldsymbol{M}$, $\boldsymbol{h}$, $\boldsymbol{g}$ are included Eq (19) that describes the dynamics of non-constraint, and those can be calculated numerically and recursively through forward dynamics calculation [6] by exploiting the inverse dynamics calculation called ‘‘Newton Euler" Method [7]. Because $\boldsymbol{M}$ is 4×4 matrix when the hyper-redundant manipulator including 4 links, resulting in a large amount of computation to calculate each element of $\boldsymbol{M}$ by using lagrange method. This implies that analytical deriving Eq (19) is almost impossible by hand writing calculation, then we utilize Newton Euler method as follows.

First of all, Eq (19) should be set as hereunder.

$$\boldsymbol{M_J}\ddot{\boldsymbol{q}} + \boldsymbol{b_J} = \tilde{\boldsymbol{\tau}} \tag{26}$$

Here

$$\begin{aligned}
\boldsymbol{M_J} &= \boldsymbol{M}(\boldsymbol{q}) + \boldsymbol{J_m} \\
\boldsymbol{b_J} &= \boldsymbol{h}(\boldsymbol{q}, \dot{\boldsymbol{q}}) + \boldsymbol{g}(\boldsymbol{q}) + (\boldsymbol{D} + \boldsymbol{D_m})\dot{\boldsymbol{q}} \\
\tilde{\boldsymbol{\tau}} &= \boldsymbol{K_m i} + \boldsymbol{j_c}^T f_n - \boldsymbol{j_t}^T f_t
\end{aligned}$$

With forward motion analysis, Eq (26) should be calculated by Newton-Euler method from the bottom link to upper link until the manipulator's hand, and also with the motion analysis of backward calculation, we get equation of motion of i-th link Eq (27).

$$\tilde{\tau}_i = {}^i\boldsymbol{z}_i^T {}^i\boldsymbol{n}_i + J_{mi}\ddot{q}_i + (D_i + D_{mi})\dot{q}_i \tag{27}$$

Therefore, the motion Eq (26) can be used to inverse dynamics calculation $\tilde{\boldsymbol{\tau}} = [\tilde{\tau}_1, \tilde{\tau}_2, \cdots, \tilde{\tau}_n]^T$ in Eq (27). This inverse calculation can be described as $\tilde{\boldsymbol{\tau}} = \boldsymbol{p}(\boldsymbol{q}, \dot{\boldsymbol{q}}, \ddot{\boldsymbol{q}}, \boldsymbol{g})$.

Then considering Eq (26) and Eq (27),

$$\boldsymbol{M_J}\ddot{\boldsymbol{q}} + \boldsymbol{b_J} = \boldsymbol{p}(\boldsymbol{q}, \dot{\boldsymbol{q}}, \ddot{\boldsymbol{q}}, \boldsymbol{g}) \tag{28}$$

Substitute $\ddot{\boldsymbol{q}} = \boldsymbol{0}$ into Eq (28):

$$\boldsymbol{b_J} = \boldsymbol{p}(\boldsymbol{q}, \dot{\boldsymbol{q}}, \boldsymbol{0}, \boldsymbol{g}) \tag{29}$$

so $\boldsymbol{b_J}$ can be calculated. Next substitute $\boldsymbol{g} = \boldsymbol{0}, \dot{\boldsymbol{q}} = \boldsymbol{0}, \ddot{\boldsymbol{q}} = \boldsymbol{e}_i (i = 1, 2, \cdots, l)$ into Eq (28), then the $\boldsymbol{b_J} = 0$:

$$\boldsymbol{m}_i = \boldsymbol{M_J}\boldsymbol{e}_i = \boldsymbol{p}(\boldsymbol{q}, \boldsymbol{0}, \boldsymbol{e}_i, \boldsymbol{0}) \tag{30}$$

here we can calculate $\boldsymbol{m}_i$ defined as the component vector of the i-th column in inertia matrix $\boldsymbol{M}$, $\boldsymbol{e}_i$ is a $l \times 1$ matrix in which the i-th element is 1 and others are all 0 like $\boldsymbol{e}_i = [0, 0, \cdots, 1_{(i)}, \cdots, 0, 0]^T$. So with Eq (30) $\boldsymbol{M_J} = [\boldsymbol{m}_1, \boldsymbol{m}_2, \cdots, \boldsymbol{m}_l]$ can be calculated one by one separately.

Thus up to now, we have calculated the $\boldsymbol{M_J}$ and $\boldsymbol{b_J}$. Back to the Eq (23), the $\boldsymbol{M}^*$ can be calculated while the constraint condition is given. Moreover, the inverse of $\boldsymbol{M}^*$ can be also calculated due to invertible for $\boldsymbol{M}^*$.

4. EVALUATION OF BRACING EFFECT

4.1 Trajectory Tracking Accuracy

In this section we compare a motion of contacting elbow on a table with the one of non-contacting on a view point of hand's trajectory tracking accuracy. The input voltage of PD controller has been set as follows.

$$\boldsymbol{v} = \boldsymbol{K_p}(\boldsymbol{q_d} - \boldsymbol{q}) + \boldsymbol{K_d}(\dot{\boldsymbol{q}}_{\boldsymbol{d}} - \dot{\boldsymbol{q}}) \tag{31}$$

$\boldsymbol{K_p}$ and $\boldsymbol{K_d}$ are both $l \times l$ positive definite diagonal matrix that indicates a position gain and a velocity gain, $\boldsymbol{q_d}$, $\dot{\boldsymbol{q}}_{\boldsymbol{d}}$ are the desired joint angle and joint angular velocity, respectively. Simulation conditions have been set as: each link's mass is $m_i = 0.3[kg]$, length is $l_i = 0.5[m]$, proportional gain is $k_{pi} = 100[V/rad]$, velocity gain is $k_{di} = 50[V * s/rad]$, viscous friction coefficient of joint is $D_i = 1.0[N * s/rad]$, torque constant is $K_i = 0.203$, resistance is $R_i = 1.1[\Omega]$, inductance is $L_i = 0.17[H]$, inertia moment of motor is $I_{mi} = 0.000164$, reduction ratio is $k_i = 3.0$, viscous friction coefficient of reducer is $d_{mi} = 0.01$ and these parameters are given by actucal motor's specufications, initial angle of joint is $(q_1, q_2, q_3, q_4) = (0.25\pi, -0.5\pi, 0.75\pi, -0.5\pi)[rad]$. Simulation time is 10[s] and numerical integration time is 10[ms].

And the trajectory has been set as a circle with radius being $0.01[m]$, with the center being $(x, y) = (0.95[m], 0.5[m])$. The desired hand's target trajectory $\boldsymbol{r}_d(t) = \boldsymbol{f}(\boldsymbol{q}_d)$ is given as,

$$\boldsymbol{r}_d(t) = \begin{bmatrix} x_d(t) \\ y_d(t) \end{bmatrix} = \begin{bmatrix} 0.25\cos\frac{2\pi}{T}t + 0.95 \\ 0.25\sin\frac{2\pi}{T}t + 0.5 \end{bmatrix} \tag{32}$$

, where $T = 5[s]$, and hand's trajectory tracking error as defined as,

$$\boldsymbol{e}(t) = \boldsymbol{r}_d(t) - \boldsymbol{r}(t) = \begin{bmatrix} e_x(t) \\ e_y(t) \end{bmatrix} = \begin{bmatrix} x_d(t) - x(t) \\ y_d(t) - y(t) \end{bmatrix} \tag{33}$$

$\boldsymbol{r}(t) = \boldsymbol{f}(\boldsymbol{q})$ is the hand's position calculated by forward kinematics. By using $\boldsymbol{r_d}(t)$ and current angle of $q_1(t)$, $q_2(t)$, q_{3d} and $q_{4d}(t)$ can be solved through kinematics as,

$$\boldsymbol{q_d}(t) = \begin{bmatrix} q_{1d}(t) \\ q_{2d}(t) \\ q_{3d}(t) \\ q_{4d}(t) \end{bmatrix} = \begin{bmatrix} q_1(0) \\ q_2(0) \\ f_3^{-1}(q_1(t), q_2(t), \boldsymbol{r_d}(t)) \\ f_4^{-1}(q_1(t), q_2(t), \boldsymbol{r_d}(t)) \end{bmatrix} \tag{34}$$

Fig.3 indicates that trajectory tracking of circle on x-y plane. The black solid line means desired hand's trajectory, and dotted line does the hand's trajectory with the robot's elbow contacting to the table, and fine dotted line does the trajectory without contacting. Since the controller of both experiments are identical, Fig.3 shows the bracing action of robot can improve the hand's trajectory tracking accuracy, what is more important is this accuracy improvement does not need any extra energy.

The following Figs. 4 and 5 are the detailed trajectory tracking errors of $e_x(t)$ and $e_y(t)$ with bracing, Fig.4, without bracing Fig.5. By comparing Fig.4 with Fig.5, it is obvious that the time average value of the $e_y(t)$ with

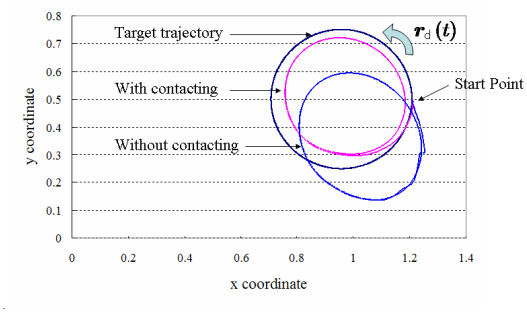

Fig. 3 Trajectory tracking of circle on x-y plane

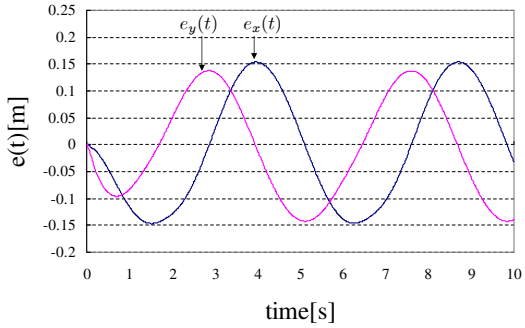

Fig. 4 Hand's trajectory tracking errors $e_x(t)$ and $e_y(t)$ with the elbow being braced

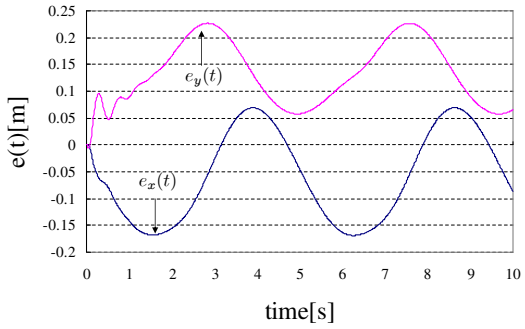

Fig. 5 Hand's trajectory tracking error $e_x(t)$ and $e_y(t)$ without bracing

bracing condition is almost zero despite the average of $e_y(t)$ without bracing being 0.15 in Fig.5. This is reasonable since the contacting of elbow can cancel the gravity force influence by reaction force given by the table naturally and without any energy consuming. Despite the motion of the hand's x-direction is vertical to the gravity compensation by the reacting force, the average of error $e_x(t)$ also decreased from -0.05 to zero, which can be seen by Figs.4 and 5. From Figs.3-5, we can say that tracking performance with contacting elbow is more accurate than non-contacting.

4.2 Influences of Bracing Position

In this section we will introduce the trajectory tracking simulation results, where the elbow's contacting position in horizontal direction varies as shown in Fig 6, in which the three initial shape of the manipulator corresponding the three elbow's contacting points are shown in the same figure. Simulation's condition has been set as:

Condition	$q_1(0)$	$q_2(0)$	$q_3(0)$	$q_4(0)$
1	0.35π	-0.7π	0.68π	-0.28π
2	0.25π	-0.5π	0.75π	-0.5π
3	0.15π	-0.3π	0.77π	-0.6π

Table 1 Initial joint angle

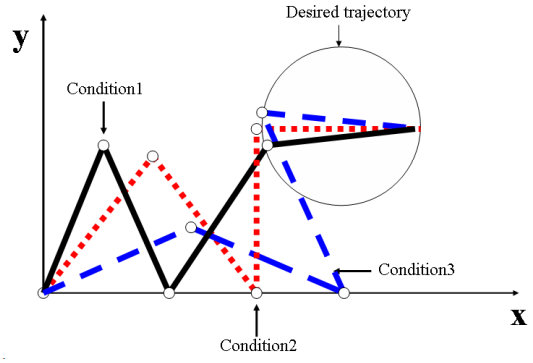

Fig. 6 Simulation condition

each link's mass is $m_i = 0.3[kg]$, length is $l_i = 0.5[m]$, proportional gain is $k_{pi} = 100[V/rad]$, velocity gain is $k_{di} = 50[Vs/rad]$, viscous friction coefficient of joint is $D_i = 1.0[Ns/rad]$, proportional constant is $K = 0.1$ to determine the radio of reaction force f_n and friction force f_t. Table 1 shows initial joint angles of $q_i(0)[rad](i = 1, 2, 3, 4)$. And the trajectory to be tracked by the hand is the same one explained in section 4.1.

Simulation results are shown in Figs.7-9. These figures describe tracking error $e_x(t)$, $e_y(t)$ of the end-effector's hand under conditions of 1-3 depicted in Fig.6.

The hand's trajectory tracking errors $e_x(t)$, $e_y(t)$ with farthest bracing point as shown "Condition 1" in Fig.6 are depicted in Fig.7, middle bracing "Condition 2" in Fig.8, nearest "Condition 3" in Fig.9.

Before examining this motion by simulations we expected that the nearest contacting bracing will get smaller tracking errors since the gravity force influence can be canceled the bulk of by nearest bracing point (Condition3). However, comparing Figs.7, 8 and 9, there appears little differences. The reason of this result may arise from our parameter setting of this simulation.

4.3 Energy Efficiencies

In this section we will introduce the energy efficiency simulation results. Link's work $W_i(T)[J]$ and power consumption $E_i(T)[J]$ used in motor's circuit of mechanical motion can be expressed as follows.

$$W_i(T) = \int_0^T \tau_i(t)\dot{q}_i(t)dt \quad (35)$$

$$E_i(T) = \int_0^T v_i(t)i_i(t)dt(i = 1, 2, 3, 4) \quad (36)$$

Moreover, summation of all link's work $W_{sum}(T)$ and summation of all power consumption $E_{sum}(T)$ can be

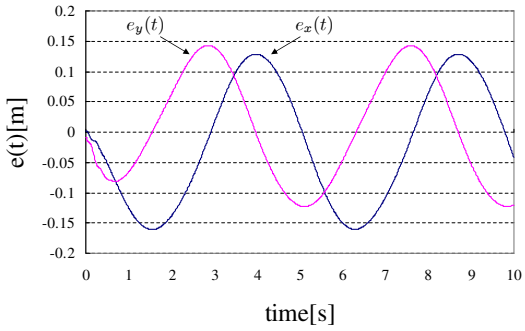

Fig. 7 $e_x(t)$ and $e_y(t)$ with farthest elbow contacting position (Condition 1)

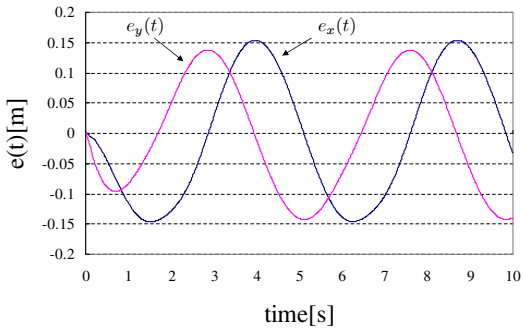

Fig. 8 $e_x(t)$ and $e_y(t)$ with middle elbow contacting position (Condition 2)

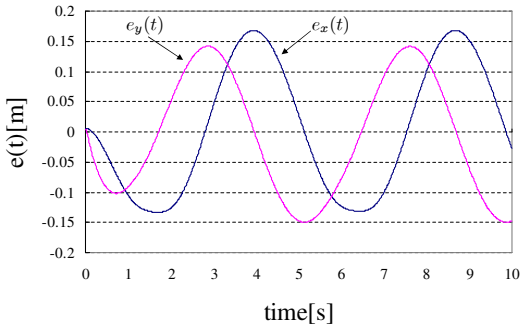

Fig. 9 $e_x(t)$ and $e_y(t)$ with nearest elbow contacting position (Condition 3)

expressed as follows.

$$W_{sum}(T) = \sum_{i=1}^{4} W_i(T) \quad (37)$$

$$E_{sum}(T) = \sum_{i=1}^{4} E_i(T) \quad (38)$$

The evaluation index is used as energy efficiency $\eta(T)$. Its definition is the ratio of input to output.

$$\eta(T) = \frac{W_{sum}(T)}{E_{sum}(T)} \quad (39)$$

Simulation's condition are all identical to the experiments in section 4.1 and 4.2 except bracing points being increased into five. Table 2 shows positions with elbow contacting, initial joint angle of $q_1(0)$ and $q_2(0)$, and Fig. 10 shows the position of contacting elbow. The target

Position with Elbow	$q_1(0)$[rad]	$q_2(0)$[rad]
$Nearest$	0.15π	-0.3π
$Near$	0.2π	-0.4π
$Middle$	0.25π	-0.5π
Far	0.3π	-0.6π
$Farthest$	0.35π	-0.7π

Table 2 Position with elbow and initial joint angle

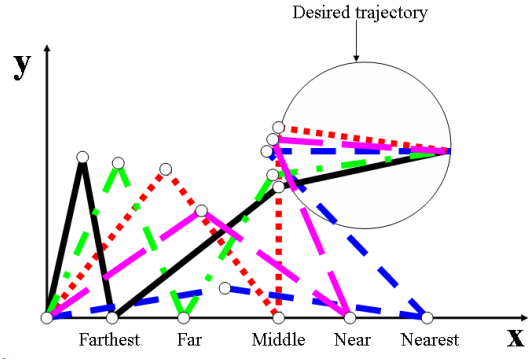

Fig. 10 Position with elbow

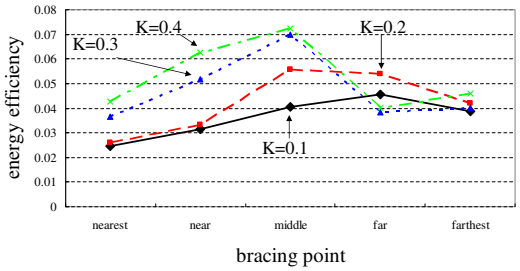

Fig. 11 Follow circular orbit

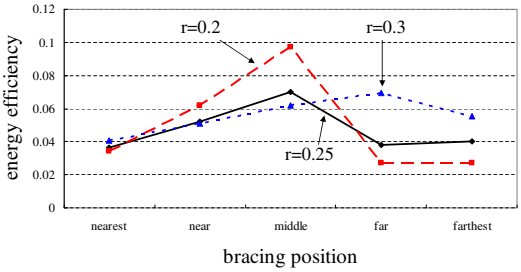

Fig. 12 Follow circular orbit

angles $q_{d1}(t)$, $q_{d2}(t)$, $q_{d3}(t)$ and $q_{d4}(t)$ is calculated by inverse kinematics from Eq (34). Figure 11 shows energy efficiency in each position with elbow contacting following circular orbit given by Eq (32).

Another target end-effector trajectory is considered as follows,

$$x_d(t) = r\cos\frac{2\pi}{T}t + 0.95 \quad (40)$$

$$y_d(t) = r\sin\frac{2\pi}{T}t + 0.5 \quad (41)$$

, in which the circle's radius r is varied as $r = 0.2, 0.25, 0.3$ as a parameters. Figure 12 shows energy efficiencies on condition of five bracing points of the elbow. From this result, it finds that the best bracing position that gives the highest efficiency is Middle for circular object.

5. CONCLUSION

In this paper, we researched on finding the best position of trajectory tracking accuracy and maximization of energy efficiency in motion control of bracing robot. We defined the motion equation of robot and motor. Compared with non-contacting, we found that tracking performance with contacting elbow is more effective. Moreover, we examined tracking accuracy and energy efficiency according to the position that the elbow attaches.

REFERENCES

[1] K. Yamamoto, "Dynamical Model of Multi-Elbow-Contacting Robot and its Effect on Hand-Trajectory Tracking Control," Master's thesis of the Graduate School of Human and Artificial Intelligent Systems, Fukui University, 2009 (in Japanese).

[2] K. Michiue, "Improvement in Position/Force Control of Grinding Robot Based on Constrained Condition," a graduation thesis of Department of Human and Artificial Intelligent Systems, Fukui University, 2008 (in Japanese).

[3] G. Wang, M. Minami, "Modeling and Control of Hyper-Redundant Mobile Manipulator Bracing Multi-Elbows for High Accuracy / Low-Energy Consumption," SICE, pp.2371-2376, 2010.

[4] M. Itoshima, "Research on Maximization of Energy Efficiency in Motion Control of Robot with Elbow," a graduation thesis of Department of System Engineering, Okayama University, 2011 (in Japanese).

[5] Y. Toda, "Evaluation of Trajectory Tracking Control of Constraint Motion concerning Elbow's Contacting Position," a graduation thesis of Department of System Engineering, Okayama University, 2011 (in Japanese).

[6] M. W. Walker and D. E. Orin, "Efficient Dynamic Computer Simulation of Robotic Mechanisms," ASME J. of DSMC,104, pp.205-211, 1982

[7] L. R. Hunt, R. Su and G. Meyer, "Global Transformation of Non Linear system," IEEE Trans. AC., 28-1, pp.24-31, 1983